

## Gold Solubility in Reduced Carbon-Bearing Fluid

A. G. Simakin<sup>a, b, \*</sup>, T. P. Salova<sup>a, \*\*</sup>, R. I. Gabitov<sup>c</sup>, L. N. Kogarko<sup>d</sup>, and O. A. Tyutyunnik<sup>d</sup>

<sup>a</sup>*Korzhinskii Institute of Experimental Mineralogy (IEM), Russian Academy of Sciences, Chernogolovka, Moscow oblast, 142432 Russia*

<sup>b</sup>*Schmidt Institute of Physics of the Earth, Russian Academy of Sciences, Moscow, 123242 Russia*

<sup>c</sup>*Department of Geosciences at Mississippi State University, Oktibbeha County, Mississippi State, MS 39762 USA*

<sup>d</sup>*Vernadsky Institute of Geochemistry and Analytical Chemistry (GEOKhI), Russian Academy of Sciences, Moscow, 119991 Russia*

\*e-mail: [simakin@iem.ac.ru](mailto:simakin@iem.ac.ru)

\*\*e-mail: [salova@iem.ac.ru](mailto:salova@iem.ac.ru)

Received June 6, 2018; revised July 26, 2018; accepted September 4, 2018

**Abstract**—The paper presents first experimental data on gold solubility in CO–CO<sub>2</sub> and C–O–S fluids with a low H<sub>2</sub>O concentration under reduced conditions, a pressure of 200 MPa, and a temperature of 950°C. Gold solubility in C–O–S fluid is approximately 27 ppm. The estimate of gold solubility in CO–CO<sub>2</sub> fluid with 10–15 mol % CO is less accurate, and the solubility is no lower than 2–3 ppm but may reach 200–300 ppm. The high gold solubility in reduced CO<sub>2</sub> fluid determined in the course of this research, and our earlier estimates of high platinum solubility (Simakin et al., 2016), may explain the deposition of mineralization of these noble metals in the Guli intrusion, polar Siberia, as a result of fluid extraction of these metals and their redeposition at a temperature slightly below the solidus. The reduction of the largely oxidized CO<sub>2</sub> fluid, which was determined using mineralogical sensors, was likely related to the subsolidus oxidation of olivine.

**Keywords:** CO–CO<sub>2</sub> and C–O–S fluids, gold, Guli Massif

**DOI:** 10.1134/S0016702919040104

### INTRODUCTION

The transfer and accumulation of gold in fluid and fluid–magmatic processes is currently thought to be related mostly to the origin of complex compounds with the Cl<sup>−</sup> and HS<sup>−</sup> negative charge anions. The solubility of gold at a high oxygen fugacity (near the MH, magnetite–hematite, buffer) is about 100 ppm, with gold dissolved in the form of Au(HS)<sub>2</sub><sup>−</sup> complexes in neutral aqueous fluid at  $T = 400^{\circ}\text{C}$  and  $P = 1$  kbar (Pokrovski et al., 2014), and decreases by roughly two orders of magnitude as the oxygen fugacity decreases to the QFM (quartz–fayalite–magnetite) buffer. It is believed that carbon in the form of CO<sub>2</sub> suppresses the solubility of gold and other metals (Van Hinsberg et al., 2016) in aqueous fluid because, for example, of its effect on the dielectric constant (Kolonin et al., 1997; Pokrovski et al., 2014). Experimental data on organometallic gold compounds at high  $P$ – $T$  parameters are still absent.

At the same time, geological observations indicate that carbon may play an important role in the mobilization and concentration of gold. A shining example of the association of PGE, gold, and carbon is offered by graphitized greenschist- to granulite-facies metamorphic rocks of the Khanka terrane. These rocks contain

0.04–62 ppm Pt and 0.02–26 ppm Au (Khanchuk et al., 2013). These authors believe that the rocks were graphitized under the effect of deep fluid and describe aggregates of graphite with Au and PGE. Intermetallic compounds of Au and Al and of Au and REE were found in nepheline syenites in central Siberia (Sazonov et al., 2008). The maximum Au concentrations were detected in graphitized rocks. High concentrations of noble metals were described in chloroform extracts from bitumoids from melilitites of the Krestovskaya intrusion: 13.4 ppm Au and 35.4 ppm Pt. The noble-metal mineralization was reportedly produced with the involvement of organosulfur compounds.

Tests of various hypotheses that deposits of noble metals are related to carbon require experimental data on the properties of Au and PGE organometallic compounds at high  $P$ – $T$  parameters. Lately first experimental data were acquired on Pt metallorganic compounds at relatively low temperatures of  $T = 200$ – $400^{\circ}\text{C}$  and  $P = 1$  kbar, with these compounds formed at reactions with asphaltenes (Plyusnina et al., 2015), and at magmatic conditions  $T = 950^{\circ}\text{C}$  and  $P = 2$  kbar in CO–CO<sub>2</sub> fluid (Simakin et al., 2016). The solubility of Au in crude oil at temperatures up to 200°C was experimentally estimated at up to 0.05 ppm (Migdisov et al., 2017). No types of Pt compounds with asphal-

tene components have been identified, and Pt solubility in fluid of CO–CO<sub>2</sub> fluid is caused by the origin of carbonyl. Along with PGE, stable naturally occurring carbonyl compounds are expected for siderophile transition metals, as was demonstrated by thermodynamic calculations for Ni (Simakin et al., 2016) and suggested for Fe, Mn, Sc, W, Cr, Mo, and V. This paper presents the first experimental data confirming that Au can significantly be dissolved in reduced carbon-bearing fluid at temperatures close to magmatic ones:  $T = 950^{\circ}\text{C}$  and  $P = 2$  kbar.

## EXPERIMENTAL

**Methods.** The experiments were carried out in an apparatus of high gas pressure at the Institute of Experiment Mineralogy, Russian Academy of Sciences. The vessel of stainless steel had a free volume of 262 cm<sup>3</sup>, the working medium was Ar. The temperature was measured during the experimental run by a Pt–Rh thermocouple, the gradient-free zone was 40–50 mm. The pressure was measured with piezo sensors accurate to 5%. The temperature and pressure were maintained accurate to  $\pm 2.5^{\circ}\text{C}$  and  $\pm 1\%$ , respectively. Quenching at a rate of 150°C/min was conducted by cooling when the furnace was switched off.

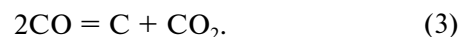
The experimental products were analyzed by microprobes: CamScan MV2300 and Tescan Vega TS5130MM equipped with an INCA Energy 450 energy-dispersive spectrometer at the Institute of Experiment Mineralogy. The Raman spectra of experimental fluid inclusions were recorded by a LabRam HR800 (Horiba, Jobin Yvon) spectrometer at Institute of Geology, Komi Research Center, Ural Branch, Russian Academy of Sciences, in Syktyvkar. The spectrometer is coupled with an Olympus BX41 optical microscope with a 50× object lens. The source of the excitation radiation was an Ar<sup>+</sup> laser (488 nm, 100 mW). Water content in experimental glasses was measured by the Karl–Fischer titration (KFT) on an Aqua 40.00 system with a high-temperature HT 1300 unit. Glasses were locally analyzed for Au by LA-ICP-MS on a Agilent 7900 quadrupole mass spectrometer equipped with a CETAC (193 nm) excimer laser at the Rochester University, United States. Bulk analysis of the samples for Au was conducted at the Vernadsky Institute by electrothermal atomic absorption spectrometry (ETAAS).

**Experimental parameters.** The fluid source in our experiments was iron carbonate. The experiments were conducted using a double-capsule method: an open smaller capsule was mounted in a gold capsule of larger diameter. The fluid source material was loaded into the smaller capsule, and the larger one contained a trap for fluid and quench phases produced at the end of the experiment. The experimental technique is described in detail in (Simakin et al., 2016). Iron car-

bonate decomposes at a temperature of 600–700°C by the reactions



Reaction (2) does not proceed completely, and minor amounts of remaining wüstite (approximately 5% of the magnetite amount) were detected in earlier experiments on determining platinum solubility (Simakin et al., 2016). Had reactions (1) and (2) proceeded completely, the initial CO concentration in the fluid would be 33 mol %, but in fact, it is lower. The maximum CO concentration is limited by the disproportionation reaction (CCO buffer)



Thermodynamic calculations predict a maximum CO content (about 21 mol %) in mixture with CO<sub>2</sub> at  $P = 200$  MPa and  $T = 1000^{\circ}\text{C}$ . The CO concentrations (measured by micro-Raman spectrometry in experimental siderite-hosted fluid inclusions) at these parameters are somewhat lower: about 15 mol % (Simakin et al., 2016). In the experiments with Pt, we got fluid inclusions entrapped in albite glass (Simakin et al., 2016). In the experiments with Au, we attempted to use sodic silicate glass, whose melting temperature is lower than that of albite glass. To dehydrate the hydroscopic sodic silicate glass, we backed it at a temperature of 250°C for 48 h. The residual water content (KFT data) was 0.93 wt %. In the course of the experimental runs, minor water amounts were transferred from the glass to dry fluid. In one of the experiments, we used a trap of quartz glass. The experimental conditions are summarized in Table 1.

Two runs were carried out with sulfur-bearing fluid at  $T = 950^{\circ}\text{C}$  and  $P = 200$  MPa. The source of sulfur was pyrite, which decomposes at a temperature of 400–450°C into pyrrhotite and gaseous sulfur. The smaller capsule was loaded with 26 mg of pyrite, and with 100 mg of sodic silicate glass was placed into the larger capsule. The starting bulk composition of the sulfur-bearing fluid was roughly estimated as follows (in mol %): CO<sub>2</sub> 50.9, CO 25.5, S<sub>2</sub> 16.0, and H<sub>2</sub>O 7.6. Because the fluid was very chemically reactive, the walls of the gold capsules were eroded in all of the experiments, and the capsules lost their hermeticity. The runs with sodic silicate glasses lasted for 2, and those with quartz glass lasted for 0.5 h. The starting oxygen fugacity in the fluid  $\log f_{\text{O}_2}$  was at the Wu–Mt buffer (near QFM – 2), and that in the hot zone of the chamber was estimated at close to the Ni–NiO (NNO + 2) buffer.

## EXPERIMENTAL RESULTS

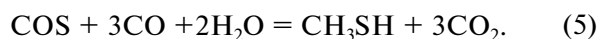
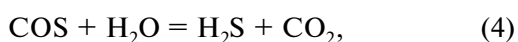
**Fluid.** The dominant sulfur species in the reduced C–O–S fluid are COS and S<sub>2</sub> at a subordinate concentration of SO<sub>2</sub>. When reacting with water, the dry fluid is hydrated with the origin of H<sub>2</sub>S and thiols (as

**Table 1.** Parameters of the experiments

Sample	Time, min	T, °C	Siderite, mg	Pyrite, mg	Glass, mg	Glass composition	Analytical technique	Au*, ppm
Ns6	30	950	60	26	100	Na <sub>2</sub> O 3SiO <sub>2</sub>	LA-ICP-MS	0.065–11.63
Ns9	30	950	60	27	100	Na <sub>2</sub> O 4SiO <sub>2</sub>	"	2.79–20.9
Ns10	30	950	60	–	105	Na <sub>2</sub> O 3SiO <sub>2</sub>	"	0.2–54
Qz94	30	950	60	–	200	SiO <sub>2</sub>	ETAAS	52.8

\* Au concentration in the trap after the experiment, range of values.

exemplified by the reaction of methanathiol synthesis below)



Characteristic lines of these components, along with those of CO<sub>2</sub>, CO, and N<sub>2</sub>, were identified in the Raman spectra of fluid inclusions hosted in the trap of sodic silicate glass. Nitrogen identified in the fluid (Fig. 1a) was obviously brought from air when the capsules were loaded. COS was identified based on a narrow band at 859.1 cm<sup>-1</sup> and a broad one at 2053 cm<sup>-1</sup>, H<sub>2</sub>S was detected based on its line at 2608 cm<sup>-1</sup>, and thiols were identified by their broad band with a maximum at 2577 cm<sup>-1</sup>. The peak of thiols has the greatest area among the peaks of all sulfur species. We failed to more accurately evaluate the concentrations because the coefficients of relative Raman cross-sections for COS and thiols are not known.

**Gold dissolution.** Early in the course of our experimental runs, fluid that was generated by siderite decomposition interacted with the walls of the capsules and dissolved gold. Figure 2 shows the surface of the gold capsule after one of our experiments. Obviously, the surface is strongly eroded, and gold is redeposited in the form of thin platelets. The fluid filled the pore space of the glass-powder trap. The powder of quartz glass was partly transformed into porous cake but was mostly not caked. Particles of the low-melting sodic silicate glass reacted with fluid and got completely fused, and quartz started to crystallize in them. These processes produced aggregate of partly recrystallized glass containing bubbles, with disseminated gold brought by fluid. The solubility of gold in the fluid can be evaluated by interpreting the glass powder with fluid as a glass trap. An analogous method of diamond trap was used to evaluate the solubility of silicate components in aqueous fluid under a pressure of a few GPa (Kessel et al., 2005). During the experiment, fluid filled the pore space of the powder and was frozen when the experimental runs were terminated. The composition of the ice with quench phases was ana-

lyzed by LA-ICP-MS. We applied an analogous approach in evaluating platinum solubility in CO–CO<sub>2</sub> fluid (Simakin et al., 2016) under the assumption that the metal was completely transferred by fluid into the trap in solution.

Optical images of the quartz particles after the experiment show a thin semitransparent gold film that reddens the surface. Gold particles about 5 μm across are concentrated at fracture corners. BSE images also show gold accumulations in fractures 50 μm long and 8–10 μm thick. The gold particles are mostly a few micrometers across, which is close to the resolution of the images. The gold is unequally distributed and is accumulated as visible clots at some particles of quartz glass. The gold was thus transferred by fluid from the walls of the gold capsule to the glass trap and the porous cake of quartz glass. The concentration of Au in the fluid can be evaluated proceeding from the starting porosity of the powder and the densities of the phases, with regard for the material balance, as is described in much detail in (Simakin et al., 2016). To do this, we analyzed three glass traps after the experiment by LA-ICP-MS for gold, sulfur, and some other elements. The analysis was conducted at the Rochester University, United States. The results are presented in Table 2.

**CO–CO<sub>2</sub> fluid.** In the run with reduced CO<sub>2</sub> fluid and sodic silicate trap, the maximum Au concentrations were detected in glass domains whose sulfur concentrations were lower than elsewhere. The starting glass contained approximately 650 ppm sulfur, which was extracted by the reduced carbon dioxide fluid (Fig. 3). This phenomenon was described in our earlier publication (Simakin et al., 2016) and may be explained by the origin of sulfur and carbon volatile compounds described above. The average gold concentration, with regard only for the lowest values, is 0.44 ± 0.25 ppm, and the maximum concentrations are 35 ± 19 ppm. The maximum concentrations pertain to analytical spots where larger gold particles occurred (see above). It is hard to unequivocally interpret the analytical data. The minimum solubility esti-

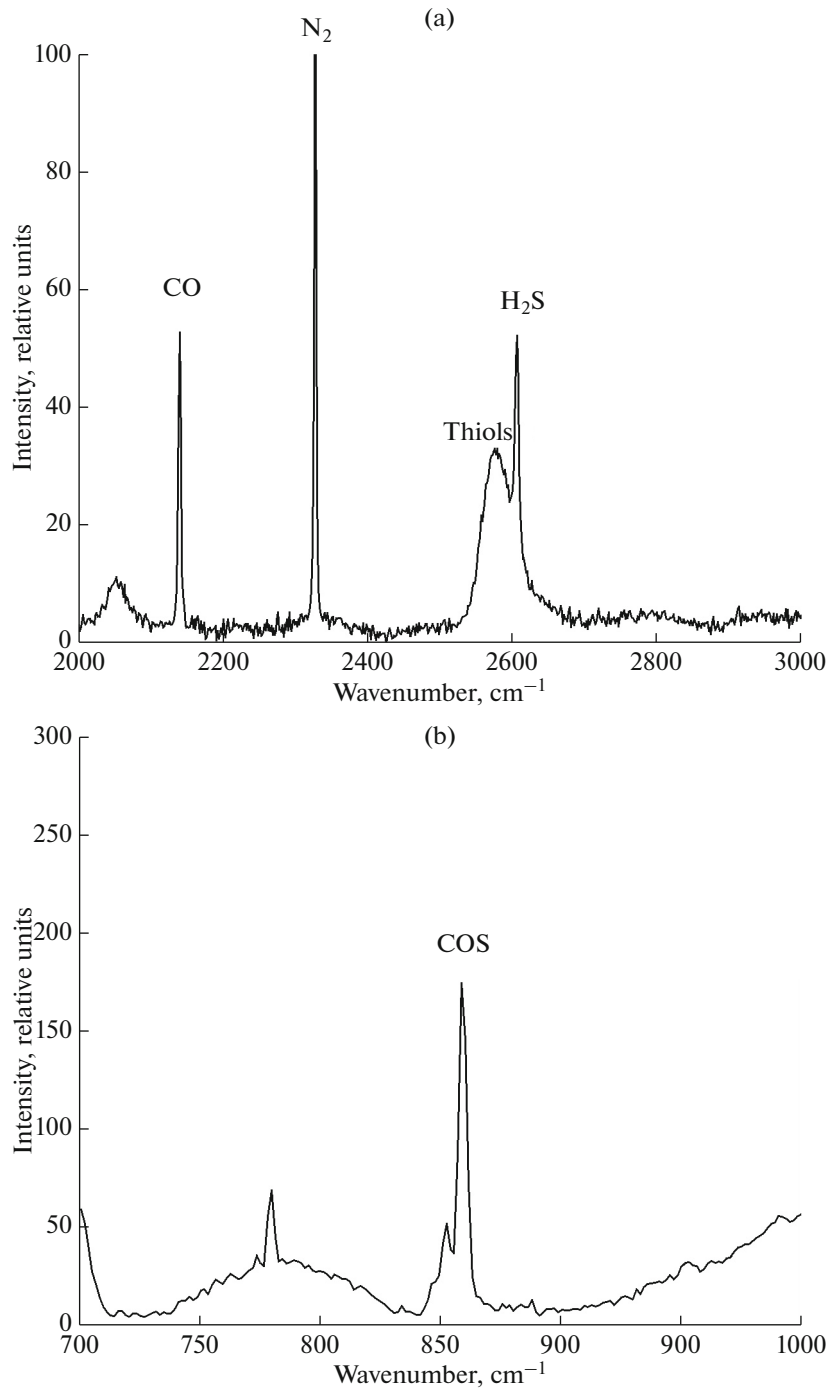


**Fig. 1.** Raman spectra of fluid inclusions in glass traps in experiments with C–O–S fluid. (a) bands of N<sub>2</sub> at 2328 cm<sup>-1</sup>, CO at 2140 cm<sup>-1</sup>, H<sub>2</sub>S at 2607 cm<sup>-1</sup>, and thiols at 2578 cm<sup>-1</sup>; (b) typical bands of COS: one narrow band at 859.1 cm<sup>-1</sup> and one broad at 2053 cm<sup>-1</sup>.

mate, which was made as in (Simakin et al., 2016), is 2–3 ppm (minimum average level). In the recalculations we used approximate values for the starting porosity  $\epsilon = 0.4$ , fluid density  $\rho_{fl} = 0.54 \text{ g/cm}^3$ , and glass density  $\rho_{gl} = 2.3\text{--}2.4 \text{ g/cm}^3$  for the sodic silicate glasses and  $2.2 \text{ g/cm}^3$  for the quartz glass, which cor-

responds to a ratio of concentrations in the fluid to trap within the range of 6–7. If the large particles were produced by condensation when the fluid reacted with the glass but not by the chemical erosion of capsule walls, then the solubility shall be higher. The maximum concentrations correspond to a solubility of about 225 ppm.

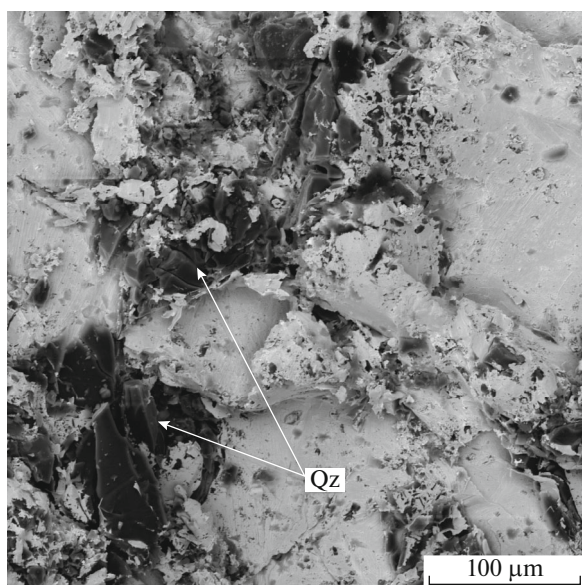


**Fig. 2.** BSE image of the inner surface of the wall of a gold capsule after an experiment with a trap of quartz glass. Black particles are quartz glass coated with redeposited gold.

In one of the runs, we used a dense cake of quartz glass that could not mechanically accommodate particles from eroded capsule walls. It is important that the cake remained permeable throughout the whole time of the experiment, whereas the trap of sodic silicate glass was eventually fused and sealed. The bulk gold concentration in the cake (ETAAS data) was 42.8 ppm. This value is close to the average value deduced from the maximum values of  $35 \pm 19$  ppm in the run with sodic silicate glass.

**C–O–S fluid.** In runs with sulfur-bearing fluid, data on gold concentrations are scattered not as widely, and gold condensation with the origin of larger particles is pronounced not as clearly. Upon rejecting two high concentration values corresponding to analyses that involved large gold particles, we obtained an average value of  $4.3 \pm 1.6$  ppm (Fig. 3). This concentration in the glass corresponds to a gold concentra-

tions in the fluid of about 27 ppm, with regard for the recalculation procedure suggested in (Simakin et al., 2016). The average for the whole dataset is  $7.3 \pm 6.2$  ppm, which corresponds to a solubility in fluid of about 45 ppm. It should be mentioned that the concentrations of gold and sulfur are positively correlated. The glass with highest gold concentration is enriched in sulfur: approximately 350 ppm.

## DISCUSSION OF EXPERIMENTAL RESULTS

The discovered high gold solubility in CO–CO<sub>2</sub> fluid is unexpected, because gold is not a transition metal, which typically can form stable carbonyls. However, the solubility of gold at  $P = 2$  kbar and  $T = 950^\circ\text{C}$  is no lower than 2–3 ppm and may be much higher (up to 300 ppm) in certain circumstances.

The determined high gold solubility in sulfur-bearing fluid is not surprising because, as has been found out previously, complexes with hydrogen sulfide

$\text{Au}(\text{HS})_n^{-(n-1)}$  with  $n$  up to 7 can be formed in aqueous fluids (Pokrovski et al., 2014) and cause a high gold solubility. Our preliminary results on gold solubility of 27–45 ppm are close the maximum values of about 100 ppm, which characterize gold solubility in the form of  $\text{Au}(\text{HS})_2^-$  complexes (Pokrovski et al., 2014).

Our system contained, along with H<sub>2</sub>S, also organosulfur compounds of the thiol type of unknown composition. Thiols were also found in low-temperature ( $T = 169$ – $195^\circ\text{C}$ ) volcanic gases of Oldoinyo Lengai sodic carbonate volcano in Tanzania (Teague et al., 2011). The volcanic gases were determined to contain, along with COS and CS<sub>2</sub>, a broad spectrum of thiols: C<sub>2</sub>H<sub>6</sub>S<sub>2</sub>, C<sub>2</sub>H<sub>6</sub>S<sub>3</sub>, C<sub>4</sub>H<sub>4</sub>S, and others [gas chromatography–mass spectrometry (GCMS) data]. Thiols of the composition C<sub>2</sub>H<sub>6</sub>S and C<sub>2</sub>H<sub>6</sub>S<sub>2</sub> were found (together with CS<sub>2</sub>) in fluid inclusions in xenoliths from Avacha volcano (GSMS data, mechanical opening of inclusions) (Sharapov et al., 2017).

## GEOLOGICAL IMPLICATIONS

As an implication of our experimental data, below we discuss a possible mechanism of the origin of native Au in the Guli ultramafic alkaline–carbonatite massif, to which a large Au and PGE placer deposit is related. The primary native gold was first found (Kogarko and Senin, 2011) in the intergranular space in dunite from the Guli Massif.

The primary meymechite magma likely contained approximately 5.8 wt % CO<sub>2</sub> and 1.8 wt % H<sub>2</sub>O (Sobolev et al., 2009). During the derivation of this magma at a depth of 200 km, the oxygen fugacity was (according to an estimates on the basis of the V/Sr ratio) close to the QFM buffer (Sobolev et al., 2009).

Thermodynamic analysis of mineral equilibria in dunites of the Guli Massif made it possible to develop

**Table 2.** Sulfur and gold concentrations (ppm) in the sodic silicate glass traps

Sample	S	Au	Sample	S	Au
Ns6	625	0.065	Ns10	636	0.88
	620	0.103		675	0.562
	781	6.32		601	0.362
	881	2.45		643	0.347
	962	11.63		640	0.2
Ns9	870	5.96	644	0.26	
	806	2.79	612	15.6	
	905	3.86	617	34.4	
	822	4.33	602	54	
	959	20.9			

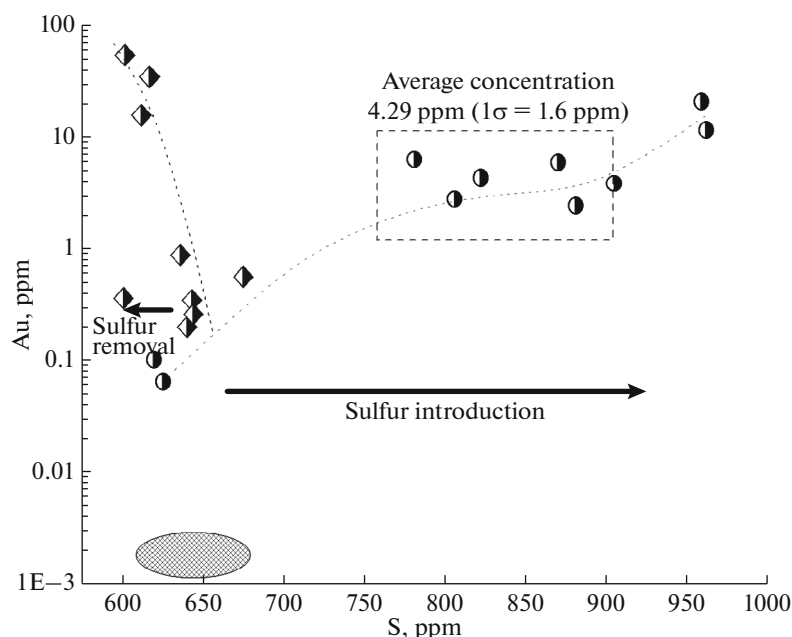


**Fig. 3.** LA-ICP-MS analyses of the trap glasses. Lozenges correspond to the run with CO–CO<sub>2</sub> fluid, circles show the results of the runs with C–O–S fluid, arrows indicate the introduction and removal of sulfur from the melt, respectively, the oval indicates the likely gold and sulfur concentrations in the starting glasses.

a new spinel–olivine–clinopyroxene oxybarometer (Ryabchikov et al., 2010). Its application has shown that the dunite was formed at fairly high oxygen fugacity of 3–2.5 logarithmic units above the QFM buffer at 1200–1300°C. These data are in good agreement with earlier estimates for the meymechites and high-Mg rocks of the Guli Massif (Ryabchikov et al., 2012).

Our research has shown that gold in dunites of the Guli Massif was produced during the late evolution of the magmatic system, in close association with sulfides, including pentlandite [whose composition varies from (Fe<sub>4.73</sub>Ni<sub>4.29</sub>Cu<sub>0.06</sub>)S<sub>8</sub> to (Fe<sub>4.33</sub>Ni<sub>4.65</sub>Cu<sub>0.02</sub>)S<sub>8</sub>], monosulfides solid solution (mss) of Fe and Ni sulfides [composition from (Fe<sub>0.57</sub>Ni<sub>0.41</sub>Cu<sub>0.09</sub>)S to (Fe<sub>0.33</sub>Ni<sub>0.66</sub>Cu<sub>0.007</sub>)S], and heazlewoodite [(Ni<sub>2.80</sub>Fe<sub>0.15</sub>Cu<sub>0.007</sub>)S<sub>2</sub>, (Ni<sub>2.73</sub>Fe<sub>0.10</sub>Cu<sub>0.01</sub>)S<sub>2</sub>]. Oxygen fugacity during the late evolution of the dunite complex was estimated for equilibrium of sulfides, iron-bearing gold, and magnetite. The calculated values show that, when the Guli intrusion cooled, the oxygen fugacity drastically dropped (Ryabchikov et al., 2016). In CO<sub>2</sub>-dominated fluid, oxygen fugacity is limited by the CCO buffer (reaction C + CO<sub>2</sub> = 2CO). The Au<sub>0.95</sub>Fe<sub>0.05</sub> + Mt equilibrium association corresponds to the oxygen fugacity of the CCO buffer ( $P = 1–2$  kbar) at a temperature of about 900°C. The equilibrium mss = Ni<sub>2</sub>S<sub>3</sub> + Mt is reached at oxygen fugacity of the CCO buffer ( $P = 1–2$  kbar) at a temperature close to 700°C. Hence, gold crystallized in the Guli intrusion from fluid at relatively high temperatures, higher than 700–900°C. Native Au in the form of Au–Ag–Cu alloy can also be formed at serpentinization of ultra-

mafic rocks with the involvement of H<sub>2</sub>O–CO<sub>2</sub> fluid at lower temperatures of 700–300°C (Palyanova et al., 2018; Murzin et al., 2018).

Carbon dioxide fluid, which can be formed by decarbonization reactions and escapes from the melt, is a strong oxidizer: at  $T = 1000^\circ\text{C}$  and  $P = 2$  kbar, the oxygen fugacity of pure CO<sub>2</sub> is on the level of NNO + 4 (Simakin et al., 2012). This seems to explain the high oxygen fugacity at the crystallization of meymechite magma in the Earth's crust. The fluid is reduced at subsolidus temperatures due to reactions between CO<sub>2</sub> and olivine.

Olivine in the dunite contains Fe<sup>2+</sup>. When fluid reacts with olivine, Fe<sup>2+</sup> in the mineral is oxidized and gives rise to magnetite-enriched spinel, and CO<sub>2</sub> is simultaneously reduced mostly to CO. Methane and other hydrocarbons occur in subordinate amounts at high temperatures. In the presence of sulfur, thiols can be synthesized. Silica is removed with fluid, and its solubility in the presence of alkalis seems to have been relatively high



The pressure under which the Guli Massif crystallized is unknown. The large size of this intrusion and the high olivine content in its dunites, as is typical of accumulates, suggest that the intrusion crystallized at depths of no less than 5–7 km. At  $T = 900^\circ\text{C}$ ,  $P = 2$  kbar, and oxygen fugacity close to QFM – 1.5, the fluid contained approximately 20 mol % CO. The generated CO is a good solvent for both PGE and Au. As the temperature decreased, CO concentration in

the fluid decreased because of disproportionation reaction (3) and methane synthesis



Fluid oxidation at its interaction with the host rocks could also be responsible for the decrease in the CO concentration. Because of this, carbonyl complexes of Au and PGE decomposed, and the released metals could be concentrated in economic quantities.

## CONCLUSIONS

The first ever data are acquired on a noticeable Au and PGE solubility in carbon-bearing fluid. This may explain the close association of these noble metals in various geological settings. The evolution of the ultramafic alkaline-carbonatite magma system of Polar Siberia was associated with a decrease in the oxygen fugacity, which triggered the transfer and redeposition of Au and PGE during the late magmatic evolution. The concentrations of the metals could then reach economic values.

## ACKNOWLEDGMENTS

The authors thank S.I. Isaenko (Institute of Geology, Komi Research Center, Ural Branch, Russian Academy of Sciences) for recording the Raman spectra. A.N. Nekrasov (Institute of Experimental Mineralogy, Russian Academy of Sciences) is thanked for conducting high-quality analysis of our experimental samples under an electron microscope. We thank Chiara Borrelli, Jacob Buettner, and Dustin Trail for helping with LA-ICP-MS analysis. The LA-ICP-MS instrument at the University of Rochester is partially supported by a grant from the Instrumentation and Facilities Program, Division of Earth Sciences, NSF [EAR-1545637]. This study was supported by the Russian Foundation for Basic Research, project no. 18-05-00597a.

## REFERENCES

R. Kessel, M. W. Schmidt, P. Ulmer, and T. Pettke, "Trace element signature of subduction-zone fluids, melts and supercritical liquids at 120–180 km depth," *Nature* **437**, (2005). doi: 10.1038/nature03971

A. I. Khanchuk, L. P. Plyusnina, A. V. Ruslan, G. G. Likhoidov, and N. N. Barinov, "Nature of graphitization and noble metal mineralization in metamorphic rocks of the Northern Khanka Terrane, Primorye," *Geol. Ore Deposits*, **55** (4), 261–281 (2013).

L. N. Kogarko and V. G. Senin, "The first find of native gold in parent rocks of the Gulinskii Massif (Polar Siberia)," *Dokl. Earth Sci.* **441** (1), 1512–1513 (2011)

G. R. Kolonin, G. A. Pal'yanova, G. P. Shironosova, and K. G. Morgunov, "The effect of carbon dioxide on internal equilibria in the fluid during the formation of hydrothermal gold deposits," *Geochem. Int.* **35**(1), 40–50 (1997).

A. A. Migdisov, X. Guo, H. Xu, A. E. Williams-Jones, C. J. Sun, O. Vasyukova, I. Sugiyama, S. Fuchs,

K. Pearce, and R. Roback, "Hydrocarbons as ore fluids," *Geochem. Persp. Lett.*, No. 5, 47–52 (2017).

V. V. Murzin, K. V. Chudnenko, G. A. Palyanova, D. A. Varlamov, E. A. Naumov, and F. Pirajno, "Physicochemical model for the genesis of Cu–Ag–Au–Hg solid solutions and intermetallics in the rodingites of the Zolotaya Gora gold deposit (Urals, Russia)," *Ore Geol. Rev.* **93**, 81–97 (2018).

G. A. Pal'yanova, V. V. Murzin, T. V. Zhuravleva, and D. A. Varlamov, "Au–Cu–Ag mineralization in rodingites and nephritoids of the Agardag ultramafic massif (southern Tuva, Russia)," *Russ. Geol. Geophys.* (3), 238–256 (2018).

L. P. Plyusnina, T. V. Kuz'mina, G. G. Likhoidov, and N. N. Barinov, "Pt behavior in the Pt–C–S ± Fe–H<sub>2</sub>O system at 200–400°C and  $P_{\text{tot}}=1$  kbar: experimental results," *Geochem. Int.* **53**(7), 581–589 (2015).

G. S. Pokrovsky, N. N. Akinfiev, A. Y. Borisova, A. V. Zotov, and K. Kouzmanov, "Gold specialion and transport in geological fluids: insights from experiments and physical-chemical modeling," *Gold-Transporting Hydrothermal Fluids in the Earth's Crust*, Ed. by P. S. Garofalo and J. R. Ridley, *Geol. Soc. Sp. Publ.* **402**, 9–70 (2014).

I. D. Ryabchikov and L. N. Kogarko, "A new version of the spinel–olivine–pyroxene oxybarometer and extreme redox differentiation in magmatic systems of mantle sources," *Dokl. Earth Sci.* **430** (6), 248–251 (2010).

I. D. Ryabchikov and L. N. Kogarko, "Oxygen potential and PGE geochemistry of alkaline–ultramafic complexes," *Geol. Ore Deposits* **54** (4), 291–304 (2012).

I. D. Ryabchikov, L. N. Kogarko, A. M. Sazonov, and N. N. Kononkova, "Formation of gold mineralization in ultramafic alkalic magmatic complexes," *Dokl. Earth Sci.* **468** (6), 623–625 (2016).

A. M. Sazonov, E. A. Zvyagina, S. I. Ient'ev, M. V. Vol'f, T. V. Poleva, V. S. Chekushin, and N. V. Oleinikova, "Associations of micro- and nano-sized segregations of noble metal complex in the ores," *Zh. SFU Tekhn. Tekhnol.* **1** (1), 17–32 (2008).

V. N. Sharapov, G. V. Kuznetsov, T. Yu. Timina, A. A. Tomilina, and K. V. Chudnenko, "Simulation of nonisothermal metasomatism of peridotite from mantle wedge beneath the Avacha group of volcanoes (Kamchatka)," *Russ. Geol. Geophys.*, No. 5, 551–570 (2017).

A. G. Simakin, T. P. Salova and G. V. Bondarenko, "Experimental study of magmatic melt oxidation by CO<sub>2</sub>," *Petrology* **20** (7), 593–606 (2012).

A. G. Simakin, T. P. Salova, R. I. Gabitov and S. I. Isaenko, "Dry CO<sub>2</sub>–CO fluid as an important potential deep Earth solvent," *Geofluids* **16**, 1043–1057 (2016).

A. V. Sobolev, D. V. Kuzmin, K. N. Malitch, and A. G. Petrunin, Siberian meimechites: origin and relation to flood basalts and kimberlites, *Russ. Geol. Geophys.*, No. 12, 999–1033 (2009).

A. J. Teague, J. Hanley, T. M. Seward, and F. Reutten, "Trace-element distribution between coexisting aqueous fumarole condensates and natrocarbonatite lavas at Oldoinyo Lengai volcano, Tanzania," *Volcanism and Evolution of the African Lithosphere*, Ed. by L. Becaluva, G. Bianchini, and M. Wilson, *GSA Spec. Pap.* **478**, 159–172 (2011).

V. J. Van Hinsberg, K. Berlo, A. A. Migdisov, and A. E. Williams-Jones, "CO<sub>2</sub>-fluxing collapses metal mobility in magmatic vapour," *Geochem. Persp. Lett.*, No. 2, 169–177 (2016).

Translated by E. Kurdyukov